

Supplementary information for

Overcoming the bottleneck of d-Band Holes in Plasmonic Photocatalysis through Molecular Electronic Coupling

*Reha Panigrahi,^a Sohini Khan,^a Prashant Sharma,^a Sakshi Kuber,^a Gayatri Joshi,^a Anirban
Mondal,^{*a} and Saumyakanti Khatua^{*a}*

^a Department of Chemistry, Indian Institute of Technology Gandhinagar, Gujarat, India

*Email: amondal@iitgn.ac.in, khatuask@iitgn.ac.in

1. Change in the local temperature of gold nanorods:

We estimated the steady-state temperature increase is given by:

$$\Delta T = \frac{Q_{abs}}{4\pi\beta R\kappa} \quad \text{----- (1)}$$

Where Q_{abs} is the absorbed power, β is the dimensionless thermal capacitance coefficient, R is the radius of a sphere having a volume equivalent to that of the nanorod, and κ is the thermal conductivity of the surrounding medium (water).

In our calculations, $\kappa = 0.6 \text{ W m}^{-1}\text{K}^{-1}$, $\beta=1.5$, and $R=14.8 \text{ nm}$, corresponding to a nanorod with an average length of 50 nm and diameter of 20 nm.

The absorbed power Q_{abs} is obtained from:

$$Q_{abs} = \sigma_{abs} \cdot I$$

Where σ_{abs} is the absorption cross-section and I is the illumination intensity. From COMSOL simulations, σ_{abs} was found to be 813 nm^2 and 5269 nm^2 at 488 nm and 633 nm, respectively. The illumination intensity was 1.45 W/cm^2 .

Using equation (1), the local temperature rise was calculated to be $71 \text{ }\mu\text{K}$ and $460 \text{ }\mu\text{K}$ at 488 nm and 633 nm, respectively. We note that the local temperature rise is too small to cause any significant enhancement of chemical reaction.

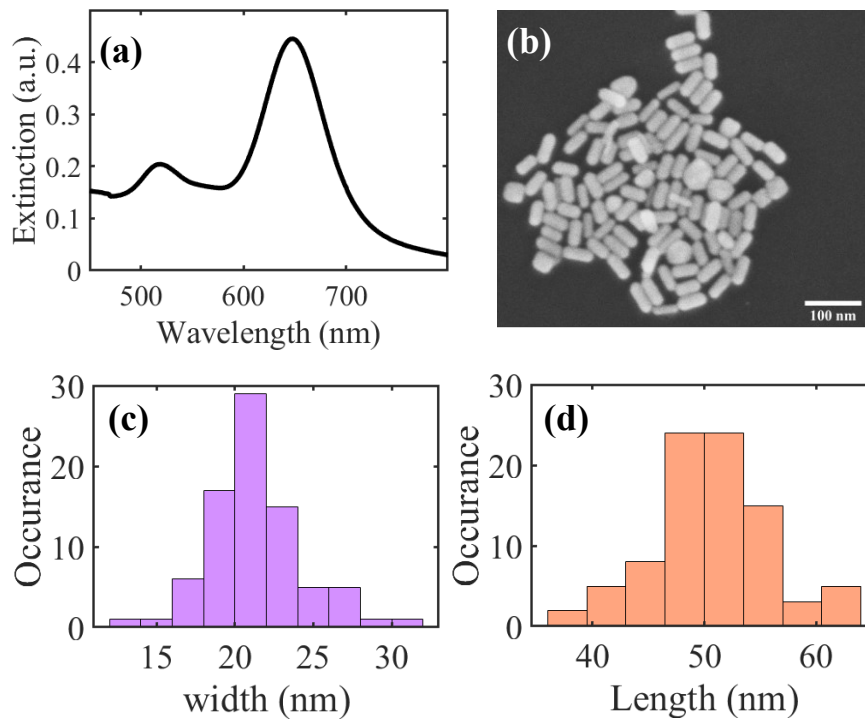


Figure S1: (a) Vis-NIR extinction spectrum of synthesized CTAB-coated gold nanorods dispersed in aqueous medium, showing a transverse surface plasmon resonance (TSPR) peak at 518 nm and a longitudinal surface plasmon resonance (LSPR) peak at 650 nm. (b) SEM image of the synthesized nanorods. (c) Histogram of the measured width distribution and (d) histogram of the measured length distribution of the nanorods, obtained from the SEM image.

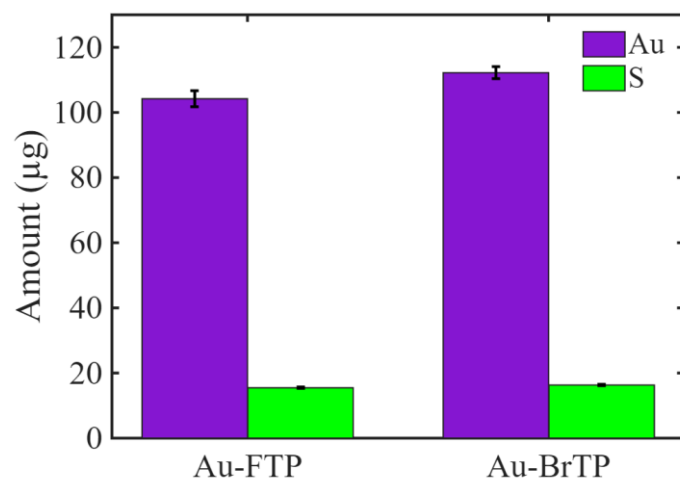


Figure S2: Quantitative estimation of Au and S from ICP-OES analysis of Au-FTP and Au-BrTP having similar OD.

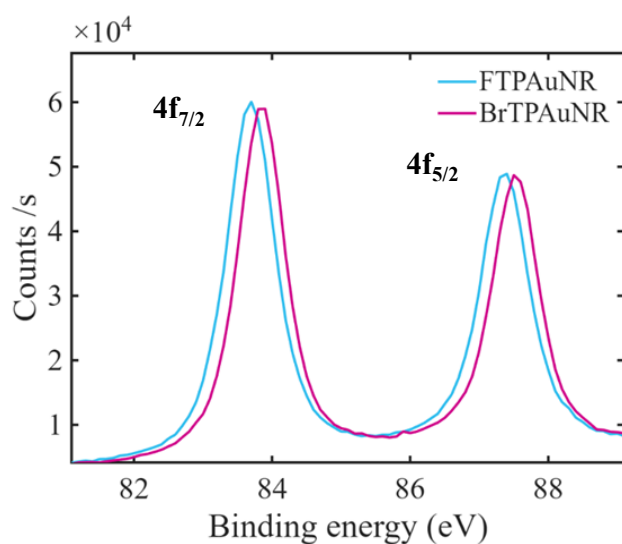


Figure S3: X-ray Photoelectron Spectroscopy (XPS) analysis of Au-FTP and Au-BrTP to verify the oxidation state of Au on the surface.

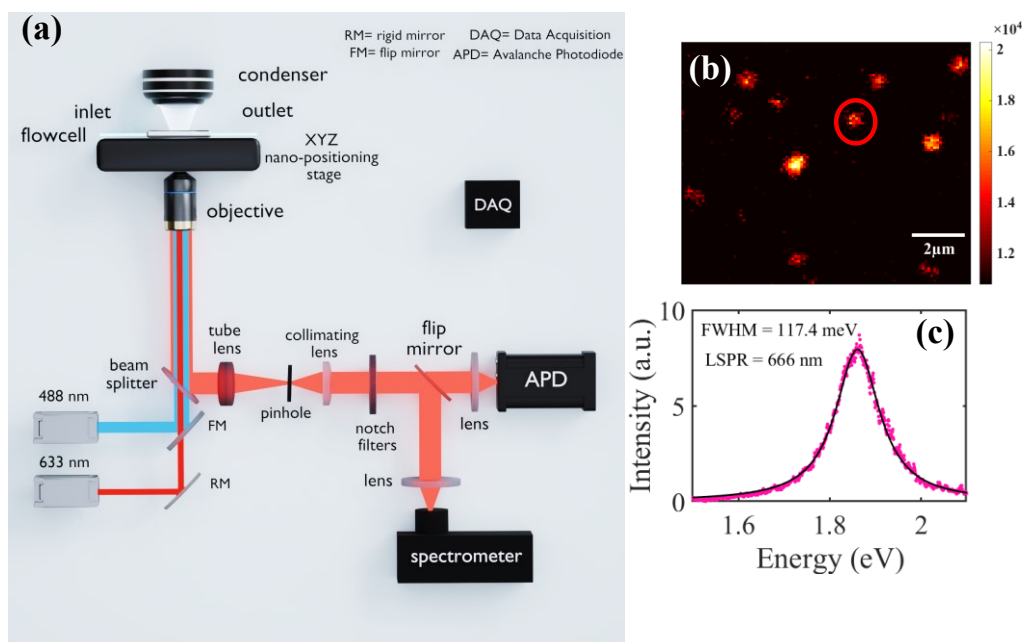


Figure S4: (a) Schematic of the dark-field microscopy setup integrated with 488 nm and 633 nm lasers for wide-field illumination. The reaction was conducted in a custom-built flow cell positioned on an XYZ nano-positioning stage. Wide-field illumination was achieved by focusing the laser at the back aperture of the objective using a 400 mm lens before the microscope. The scattering image was recorded by an avalanche photodiode (APD), while the corresponding spectrum was collected using a spectrometer. (b) APD image of light scattered by single nanorods. (c) A representative spectrum of a single gold nanorod (highlighted with a red circle), fitted using a Lorentzian function to determine the full width at half maximum (FWHM) and plasmon resonance peak position. DAQ: Data Acquisition Board.

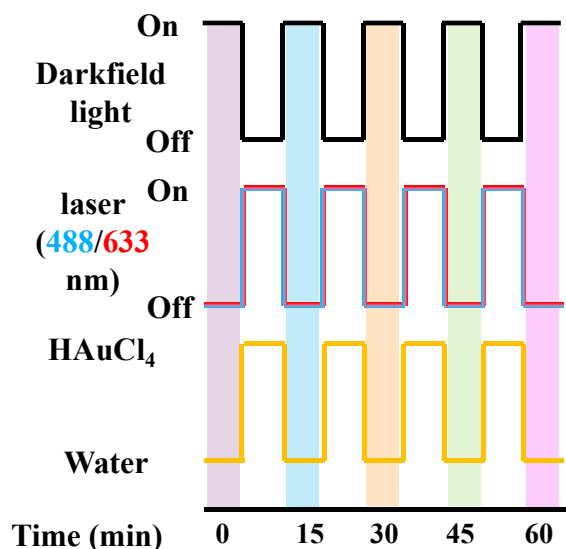


Figure S5: Schematic of sequential experimental conditions followed in single particle DFS studies.

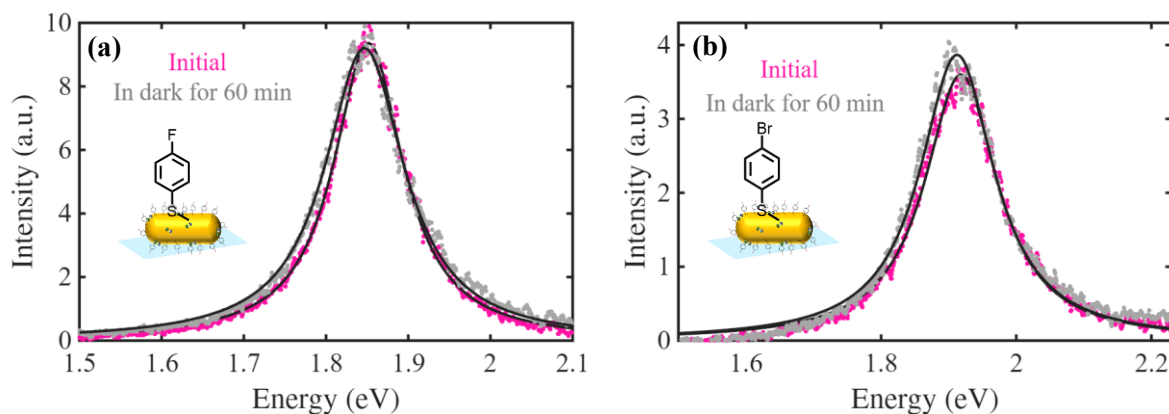


Figure S6: Scattering spectra of (a) Au-FTP and (b) Au-BrTP recorded initially (magenta) and after 60 minutes of incubation in HAuCl_4 in the dark (grey)

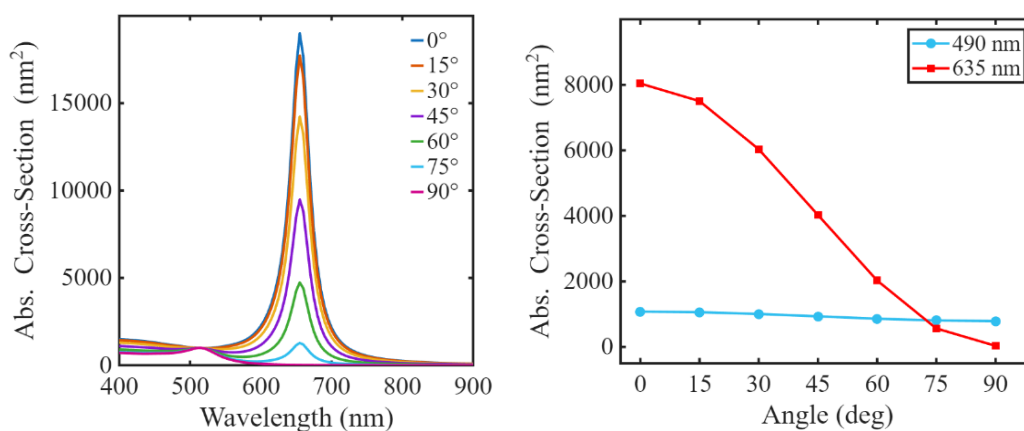


Figure S7: (a) Simulated absorption cross-section spectra of a gold nanorod ($50 \times 20 \text{ nm}$) under linearly polarized light at different polarization angles. (b) Guide to the eye illustrating the variation in absorption cross-section at 490 nm (blue) and 635 nm (red).

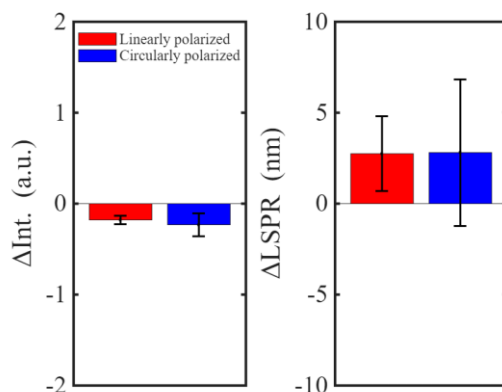


Figure S8: Comparison of the change in (b) intensity and (c) wavelength on Au^{3+} reduction for 60 min under linearly (red) and circularly (blue) polarized illumination.

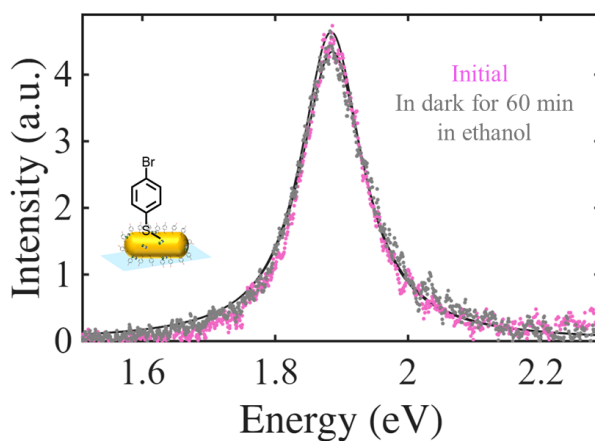


Figure S9: Scattering spectra of Au-BrTP recorded initially and after 60 minutes of incubation in ethanolic HAuCl_4 in dark (grey).

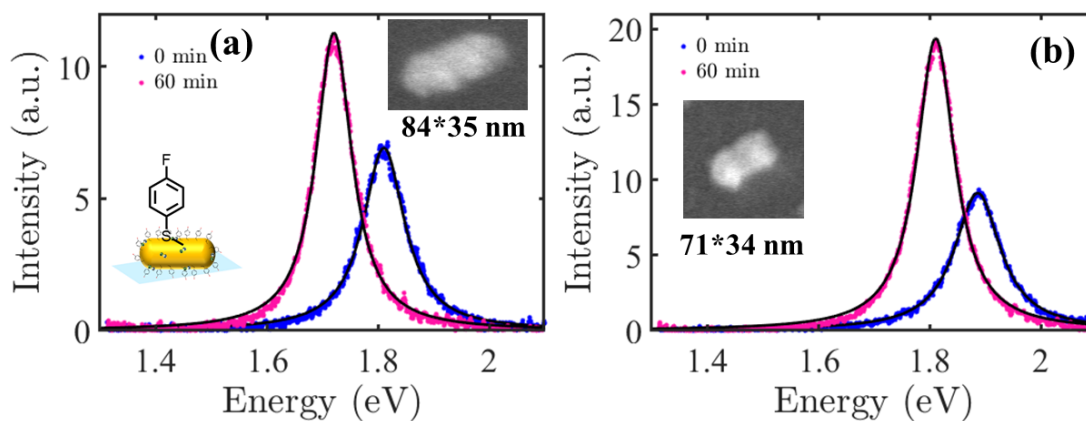


Figure S10: (a,b) Scattering spectra of Au-FTP before (blue) and after (magenta) Au deposition induced by interband (488 nm) irradiation. Insets show the corresponding SEM images of the nanorods after Au deposition.

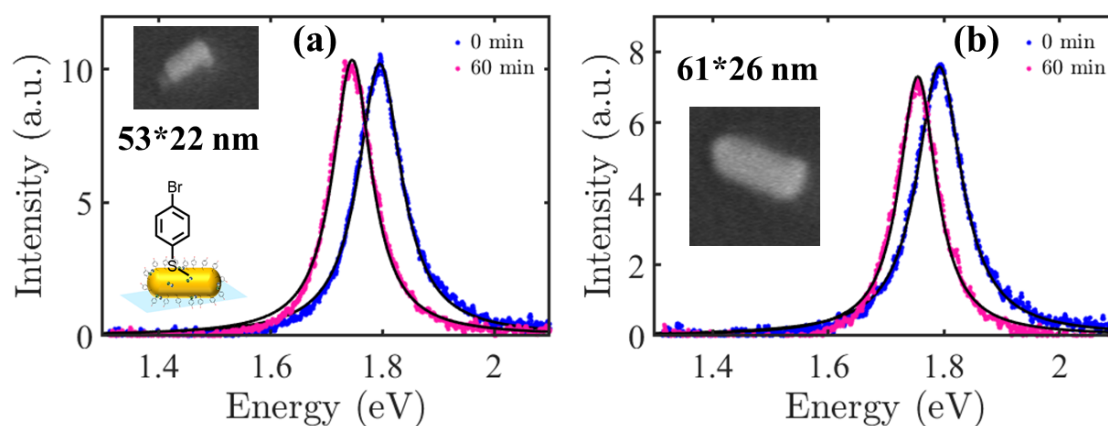


Figure S11: (a,b) Scattering spectra of Au-BrTP before (blue) and after (magenta) Au deposition induced by interband (488 nm) irradiation. Insets show the corresponding SEM images of the nanorods after Au deposition.

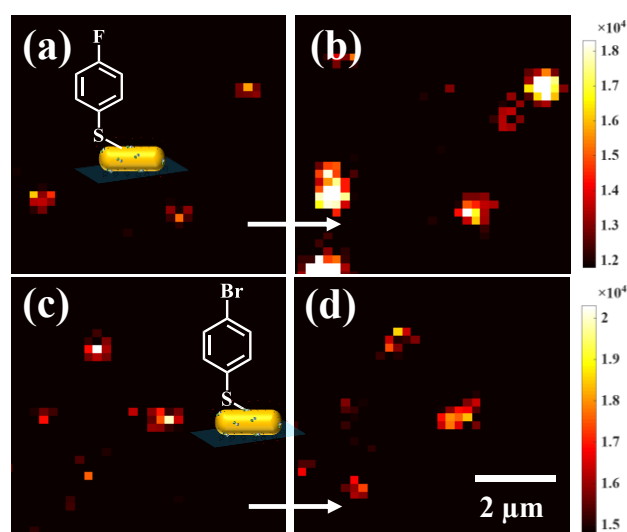


Figure S12: Darkfield scattering image of Au-FTP (a) before and (b) after Au^{3+} photoreduction to Au^0 on the surface. The image acquired after Au deposition shows high scattering intensity, signifying significant deposition. On the other hand, deposition on Au-BrTP (c) before and (d) after shows no significant difference in the intensity.

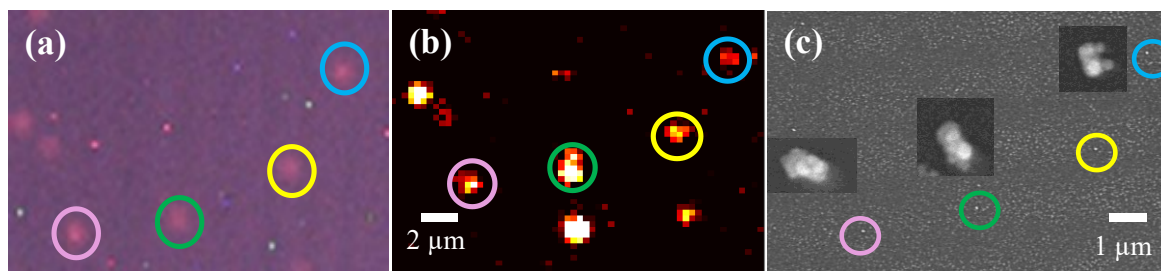


Figure S13: Correlation between (a) the dark-field scattering image captured with the camera, (b) the corresponding image captured by the APD, and (c) the same area imaged using SEM (inset shows the zoomed-in image of Au-FTP after Au⁰ deposition).